JOURNAL OF APPLIED ELECTROCHEMISTRY 11 (1981) 69–75

# *A new type of organic electrosynthesis reactor with a two-phase gas-electrolyte stream flowing through a mercury cathode. II. Limiting currents and mass-transfer studies in organotin electrosynthesis*

A. SAVALL, J. MAHENC

*Laboratoire de Chimie-Physique et Electrochimie, Associé au CNRS, Université Paul-Sabatier, 118 route de Narbonne, 31077 Toulouse, France*

G. LACOSTE

*Laboratoire de Recherche et Développement en Génie Chimique, Associé au CNRS, Institut du Génie Chimique, Chemin de la Loge, 31078 Toulouse, France*

Received 17 March 1980

A new electrochemical reactor involving a mercury cathode and a two-phase (gas–liquid) flow has been studied with a view to continuously manufacturing hexaphenyl and hexabutyldistannane by reduction of triorganotin chloride $R_3SnCl$. In each case the interpretation of the determining step of the process is discussed after a study of the electrochemical kinetics. In the reactor an efficient renewal of the cathodic surface is obtained by passing the electrolysis solution together with nitrogen gas through the mercury pool. Results of mass transfer rate studies with the cell working either as a plug–flow reactor or as a continuously stirred reactor are compared for different gas and electrolyte flows. The experiments show that gas and electrolyte flows through a mercury pool offer attractive possibilities of application for large-scale preparative electrolysis, by solving simultaneously the problems of mass transport and electrode surface renewal.

## 1. Introduction

In electrolysis plants using a mercury-pool electrode the use of a circulating solution is a good means of solving the mass transfer problem while at the same time providing for renewal of the electrode surface. Besides these advantages, electrolysis with a circulating solution offers the well-known possibility of constructing cells for continuous electropreparation [1–6]. On the other hand, interest has been expressed recently in the enhancement of mass transfer at an electrode by gas stirring [7–14]. Ibl *et al.* [7] have examined gas-stirred cells and have pointed out that gas sparging is an efficient and economic means of stirring an electrolyte.

In a previous paper [15], the idea was introduced of employing an electrolyser with a mercury-pool cathode lying on a fritted glass disc through which passes a two-phase stream of inert gas and electrolyte. Using this technique on a small-scale device, it was demonstrated that the continuous electropreparation of distannanes such as $Ph_3SnSnPh_3$ or $Bu_3SnSnBu_3$ is readily performed. In order to predict the overall size of the electrode required to manufacture these products at a given rate, it seems worthwhile to study the mass transport characteristics of such a two-phase flow cell. For this purpose it is necessary to know how the kinetics of the electrode reaction depends on the concentrations of the reactants and on the flow rates of gas and electrolyte. This paper reports an experimental investigation of the mass transfer problem for two operating modes of the reactor: the continuously stirred reactor (CSR) and the plug–flow reactor

0021–891X/81/010069–07$02.70/0  

(PFR) [15]. The study is limited to $Ph_3SnCl$ and $Bu_3SnCl$ reductions in methanol to test the mass transfer behaviour of the reactors.

## 2. Electrolysis cell

### 2.1. *The two-phase flow cell and its operation*

The experimental conditions, in particular the position of the mercury cathode in the cell, the external circuit, the electrolyte chosen and the working potentials correspond closely to those described previously in Part I [15]. The electrochemical reactor was also described there. Experiments were carried out with the reactor operating in two modes: PFR and CSR.

### 2.2. *Comparison with a traditional mercury pool*

To allow comparison of mass transport between mercury agitated by electrolyte and/or gas flows, and mercury mechanically agitated, a similar, but smaller cell (100 $cm^3$ of catholyte) with a 20 $cm^2$ area cathode, magnetically stirred, was used to record polarization curves.

## 3. Mass transport characteristics and measurements

### 3.1. *General considerations*

Diffusion and forced convection are the two modes of mass transfer whose rate may be determined by measurement of the limiting current for the cathodic reduction. In the presence of an excess of supporting electrolyte the transport of the reactant to the interface depends on its diffusion coefficient as well as on the prevailing hydrodynamic conditions.

The mass transfer rate $N$ at the electrode is related to the current $I$ by the relation

$$I = nFAN = nFAk(C - C_{el})$$

where $nF$ is the quantity of electricity per mole involved in the reaction, $A$ the effective surface area of the electrode, $k$ the mass transfer coefficient and $C$ the reactant concentration in the bulk solution. $C_{el}$, the concentration at the electrode, is practically zero at the limiting current $I_l$ which is given by

$$I_l = nFAkC. \quad (1)$$

On the other hand, the reduction of organohalostannanes on mercury is known to involve strong adsorption phenomena [16–23]. Now adsorption has an important influence on the kinetics of electrode reactions. In the case of the mercury electrode, the current–voltage polarographic curves do indeed show the influence of adsorption on the electrode processes [24–26]. This can be proved from the characteristic changes in the shape of the electrocapillary curves. These curves have been obtained by plotting the formation time of mercury drops (proportional to the interfacial surface tension of the liquid electrode) against the polarizing voltage.

### 3.2. *Case of $Ph_3SnCl$*

The current–voltage curves for the reduction of $Ph_3SnCl$ (Fig. 1) reveal the existence of a current plateau for potentials beyond $-2.2$ V with respect to $Ag/Ag^+$. Reduction of $Ph_3SnCl$ at this potential is a two-electron process leading to $Ph_3Sn^-$ via $Ph_3Sn^{\cdot}$, and thereafter to $Ph_3SnSnPh_3$ by chemical steps [18, 20, 22, 15]. Beyond $-2.2$ V, the electrode is operating at the diffusion-controlled limiting current.

### 3.3. *Case of $Bu_3SnCl$*

The current–voltage curve for $Bu_3SnCl$ (Fig. 2, curve 1) exhibits a diffusion plateau for the first reduction wave (A) at $-1.7$ V only for weak

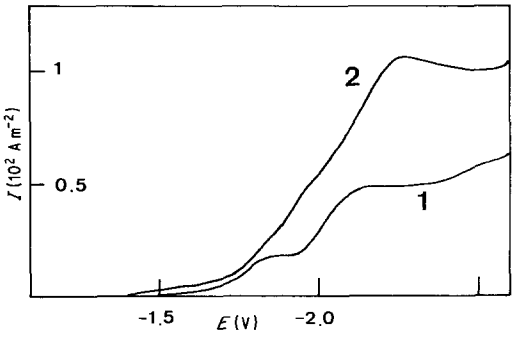


Fig. 1. Cathodic current versus potential for the reduction of $Ph_3SnCl$ on the mercury electrode in the PFR. Flow rate: electrolyte $1.68 \times 10^{-3}$ $m^3$ $s^{-1}$ $m^{-2}$; nitrogen $3.75 \times 10^{-3}$ $m^3$ $s^{-1}$ $m^{-2}$. Reactant concentration in MeOH, 0.5 M $LiClO_4$: (1) $C = 2.5 \times 10^{-3}$ mol $dm^{-3}$; (2) $C = 5 \times 10^{-3}$ mol $dm^{-3}$. Currents and flows are given for 1 $m^2$ of horizontal cross-section of the cathode. Potentials are given with respect to $Ag/Ag^+$.

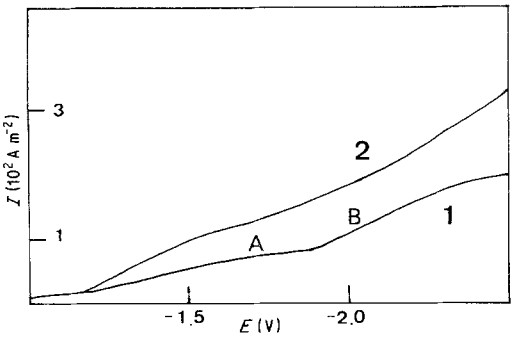


Fig. 2. Cathodic current versus potential curves for the reduction of $Bu_3SnCl$ on the mercury electrode in PFR. Flow rate: electrolyte $1.68 \times 10^{-3}$ m$^3$ s$^{-1}$ m$^{-2}$; nitrogen $3.75 \times 10^{-3}$ m$^3$ s$^{-1}$ m$^{-2}$. Reactant concentration in MeOH, 0.5 M LiCl: (1) $C = 3.7 \times 10^{-3}$ mol dm$^{-3}$; (2) $C = 7.4 \times 10^{-3}$ mol dm$^{-3}$. Currents and flows are given for 1 m$^2$ of horizontal cross-section of the cathode. Potentials are given with respect to $Ag/Ag^+$.

concentrations. The second wave (B) at $-2.0$ V, which is coalesced with the first (Fig. 2, curve 2), shows no marked diffusion plateau for concentrations up to $5 \times 10^{-3}$ mol dm$^{-3}$ which are used in electropreparations. In the latter case it is the charge transfer and not the mass transfer by diffusion which limits the overall rate of the process. This assumption will be discussed in Section 4 with the aid of polarographic studies of $Bu_3SnCl$ in methanol solution. Nevertheless, three arbitrary values for the voltage were chosen ($-1.7$ V, $-1.9$ V and $-2.1$ V) to allow comparison of the currents as functions of concentration (see Fig. 5 below).

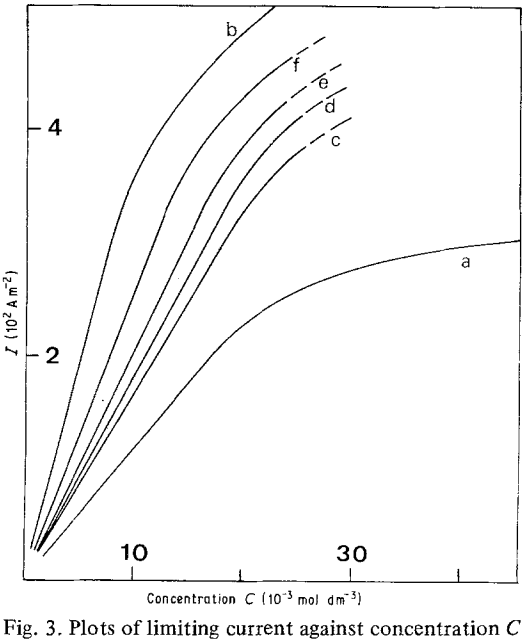


Fig. 3. Plots of limiting current against concentration $C$ of $Ph_3SnCl$ in MeOH, 0.5 M $LiClO_4$. Magnetic agitation: 2 Hz, (a) on half of the mercury pool surface (20 cm$^2$), (b) on the whole of the surface. PFR: electrolyte (gas) flow rate ($\times 10^{-3}$ m$^3$s$^{-1}$ m$^{-2}$): (c) 0.96 (3.75), (d) 1.29 (3.75), (e) 1.68 (3.75), (f) 1.68 (7.08). Currents and flows are given for 1 m$^2$ of horizontal cross-section of the cathode.

### 3.4. *Choice of the test reaction*

The mass transfer at the mercury–solution interface was studied for the case of the reduction of $Ph_3SnCl$, for which measurements of the limiting current allow the mass transfer coefficient to be calculated using Equation 1.

## 4. Relationship between current and concentration

In this study, the reactor was operated in plug-flow mode and its behaviour was compared with that observed with a mercury bath agitated by magnetic stirring.

### 4.1. *Case of $Ph_3SnCl$*

In Fig. 3 the variations in limiting current are shown as a function of the concentration in $Ph_3SnCl$ for various flow rates of nitrogen and electrolyte as well as for two different degrees of magnetic agitation. The proportionality between limiting current and concentration of the active species (Equation 1) has been verified up to a concentration of $2 \times 10^{-2}$ mol dm$^{-3}$ for $Ph_3SnCl$ (Fig. 3). At high reactant concentrations the values of the limiting current for the reduction of $Ph_3SnCl$ tend towards a limit which depends on the hydrodynamic conditions (Fig. 3). Attempts to correlate the existence of this saturation of the limiting current with adsorption phenomena such as are observed in the electropreparation of some organic compounds [27] meet with little success in the case of $Ph_3SnCl$. Indeed, the electrocapillary curve of $Ph_3SnCl$ $10^{-3}$ mol dm$^{-3}$ in methanol (Fig. 4) shows no evidence for appreciable adsorption of the final product of the reduction for working potentials more negative than $-1.85$ V with respect to $Ag/Ag^+$. So we may assume that in the case of the reduction of $Ph_3SnCl$ at a working potential of $-2.2$ V and

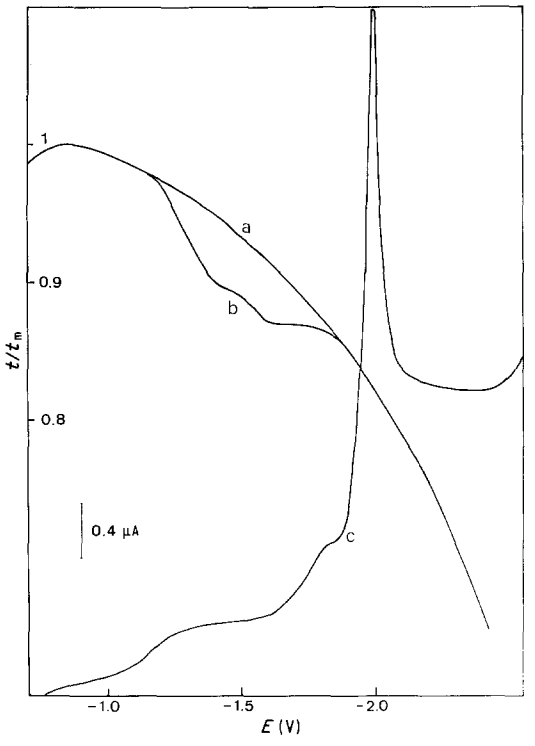


Fig. 4. Electrocapillary curve: (a) MeOH, 0.5 M $LiClO_4$; (b) $1.2 \times 10^{-4}$ mol dm$^{-3}$ $Ph_3SnCl$ in the same solution. Drop time of mercury: $t$; maximal drop time: $t_m$. (c) Polarographic current versus potential curve of the same $Ph_3SnCl$ solution (Polarograph: Metrohm E 506 polarecord).

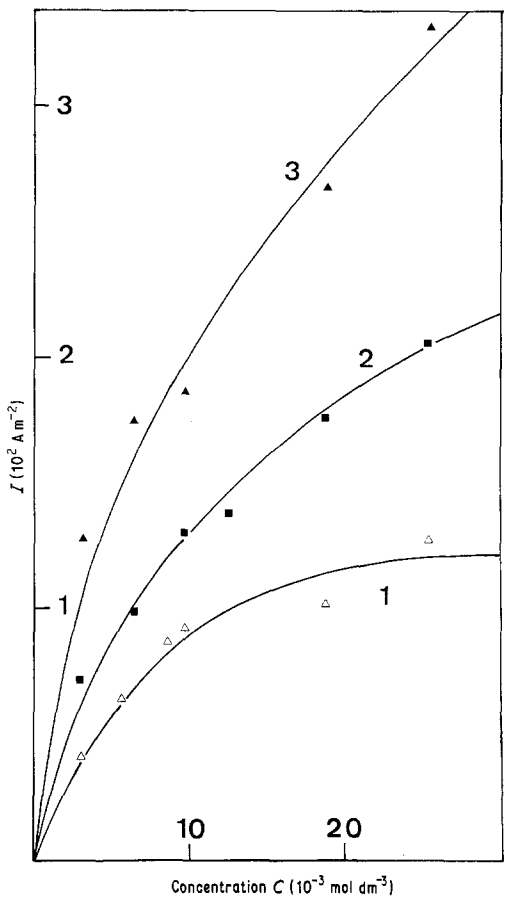


Fig. 5. Plots of current against concentration $C$ of $Bu_3SnCl$. Reduction in PFR at: (1) — 1.70 V; (2) — 1.90 V; (3) — 2.1 V (with respect to $Ag/Ag^+$) in 0.5 M LiCl, MeOH at $1.68 \times 10^{-3}$ m$^3$ s$^{-1}$ m$^{-2}$. Gas flow rate: $3.75 \times 10^{-3}$ m$^3$ s$^{-1}$ m$^{-2}$. Currents and flows are given for 1 m$^2$ of horizontal cross-section of cathode.

at concentrations greater than $2 \times 10^{-2}$ mol dm$^{-3}$ adsorption phenomena are not likely to bring about saturation of the limiting current. However, an explanation for this change in the apparent order (Fig. 3, curve a) of the reaction may be found in the formation of a coating of insoluble solid hexaphenyldistannane which masks the electrode surface; the elimination of the coating then becomes the limiting step in the process. At low $Ph_3SnCl$ concentrations ($C < 2 \times 10^{-2}$ mol dm$^{-3}$), on the other hand, the rate of removal of the product becomes greater than its rate of formation under the prevailing hydrodynamic conditions; in this case, the limiting current is once again proportional to the concentration.

### 4.2. *Case of $Bu_3SnCl$*

The variation of the current with respect to the reactant concentration for three working potentials are shown in Fig. 5. It appears that the relationship is linear only for low concentrations ($C < 0.5 \times 10^{-2}$ mol dm$^{-3}$). One possible explanation of such behaviour would be the effects of adsorption on to the mercury electrode. Indeed, the polarographic characteristics (Fig. 6) of the prewave $A_1$ and the shape of the electrocapillary curve prove that the final product of the reaction is adsorbed for working potentials up to — 2.1 V. So, for cathode working potentials less than — 1.6 V, i.e. those used in electropreparations, the currents observed are in fact always due to the reduction of the reactant $Bu_3SnCl$ through an adsorbed film which slows down the electrode process.

Furthermore, during electrolysis of solutions at high $Bu_3SnCl$ concentrations ($C > 10^{-2}$ mol dm$^{-3}$), the thickness of the film increases rapidly,

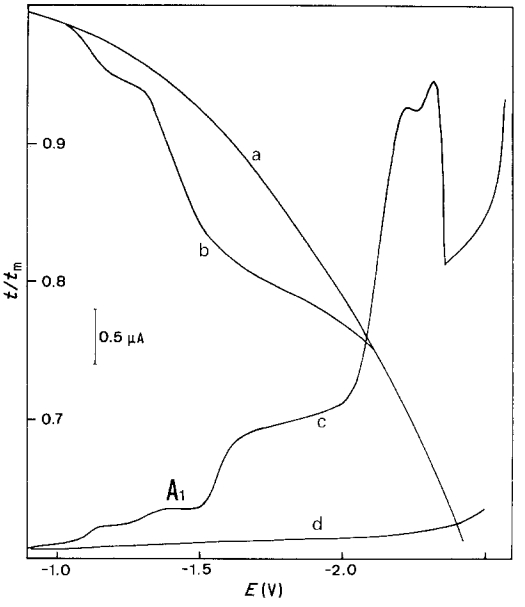


Fig. 6. Electrocapillary curve: (a) MeOH, 0.5 M $LiClO_4$; (b) $10^{-3}$ mol $dm^{-3}$ $Bu_3SnCl$ in the same solution. Drop time of mercury: $t$; maximal drop time: $t_m$. (c) Polarographic current versus potential curve of the same $Ph_3SnCl$ solution: (d) residual (Polarograph: Metrohm E506 polarecord).

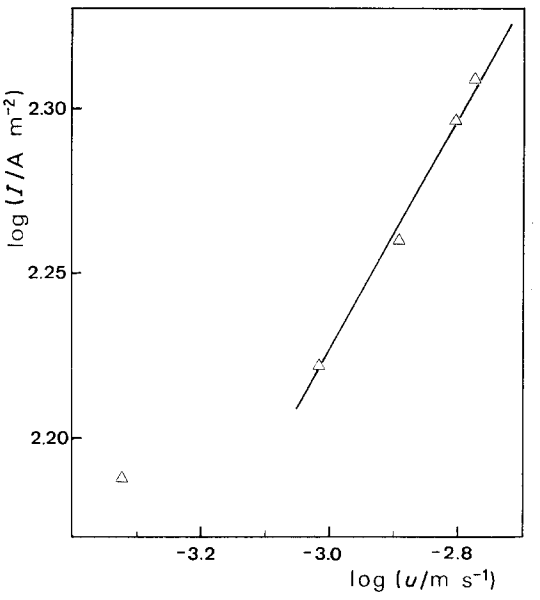


Fig. 7. Dependence of the limiting reduction current $I$ for $10^{-2}$ mol $dm^{-3}$ $Ph_3SnCl$ on liquid linear velocity $u$ for the PFR. MeOH, 0.5 M $LiClO_4$. Gas flow rate: $3.75 \times 10^{-3}$ $m^3$ $s^{-1}$ $m^{-2}$. Currents are given for 1 $m^2$ of horizontal cross-section of cathode.

and the rapid dimerization of the tributylstannyl radical $Bu_3Sn^{\cdot}$ creates a coating of insoluble liquid hexabutyldistannane, which becomes visible. Thus the current, which is controlled by diffusion for concentrations less than $5 \times 10^{-3}$ mol $dm^{-3}$ (first wave A at $-1.7$ V, curve 1 in Fig. 2) is slowed down by the surface coating substance. At concentrations above $10^{-2}$ mol $dm^{-3}$, the charge transfer is slowed to such an extent that the electrode process becomes limited by the elimination of this coating of insoluble distannane by hydrodynamic stirring.

## 5. Relationship between limiting current and flow rate of electrolyte

### 5.1. *Plug-flow reactor*

The maximum value of the Reynolds number ($Re \leqslant 160$), calculated using the diameter of the cell at the level of the mercury bath ($d = 0.1$ m), implies that, in all cases, a laminar flow regime prevails at the mercury–electrolyte interface. The two-electron reduction of $Ph_3SnCl$ was carried out to test the operation of the electrode in the flowing solution. Fig. 7 represents the logarithmic dependence of the magnitude of the limiting current on the linear velocity of the solution at constant reagent concentration and gas flow. The first point (mean linear velocity $u = 4.74 \times 10^{-4}$ m $s^{-1}$) lies off the straight line because below $9 \times 10^{-4}$ m $s^{-1}$ the electrolyte flow passes preferentially through an outer ring in which the mercury bath is thinner than in the middle because of a slight concavity in the sintered glass. When the flow rate reaches a value of about $9 \times 10^{-4}$ m $s^{-1}$, the electrolyte suddenly starts to well up across the whole surface of the mercury bath. After this change, and for concentrations of the reactant $Ph_3SnCl$ less than $2 \times 10^{-2}$ mol $dm^{-3}$, the limiting current $I_l$ is proportional to the mean velocity $u$ of the electrolyte raised to the power $0.35 \pm 0.05$:

$$I_l \propto u^{0.35}. \qquad (2)$$

The linear plots cover velocity values from $9 \times 10^{-4}$ to $1.8 \times 10^{-3}$ m $s^{-1}$. This correlation is thus consistent with the equation of Levich [28]: $I_l \propto u^n$, in which $n$ is a constant dependent on the form of the electrode. Along with velocity, the diffusional flow is a function of the geometric conditions of the flow, the viscosity and the

diffusion coefficient of the reactant. In the case of laminar flow, experimental results [29, 30] for various systems and types of operation give values for $n$ between 0.50 and 0.33.

### 5.2. *Continuously stirred reactor*

In this mode of operation, variations in the methanol flow rate have hardly any influence on the limiting reduction current when the volumetric flow rate of nitrogen is sufficient ($2.8 \times 10^{-5}$ $m^3 s^{-1}$ or $3.5 \times 10^{-3}$ $m^3 s^{-1}$ per $m^2$ of horizontal cross section of cathode) to ensure the elimination of the product formed in the electrolysis.

## 6. Relationship between limiting current and nitrogen flow rate

### 6.1. *Plug–flow reactor*

A definite increase in the value of the limiting current is observed if a nitrogen flow is superimposed on to a given electrolyte flow (Figs. 3 and 8). According to Jennings *et al.* [8], in electrolytic cells with two-phase (liquid–gas) flow, the observed mass transfer enhancement results mainly from an increase in the linear velocity of the liquid phase due to a reduction in the effective cross-sectional area due to the presence of bubbles. Thus the $I_1$ value increases as the flow rate of $n_2$ increases; however, the effect here is less significant than the hydrodynamic relationship (Equation 2) might allow us to hope. In our experiments (Fig. 8, curve b) the gas-phase volumetric flow rate was increased to just over 4.5 times the liquid volumetric flow rate, and consequently, if we assume that at the same time the linear velocity $u$ of the electrolyte should be multiplied by a factor of about 5.5, it results from Equation 2 that the limiting current must be raised by a factor of 1.82. In fact, it was observed that for a nitrogen flow rate $Q = 6 \times 10^{-3}$ $m^3 s^{-1} m^{-2}$, the current was only 1.3 times greater than that for a flow rate $Q = 1.3 \times 10^{-3}$ $m^3 s^{-1} m^{-2}$.

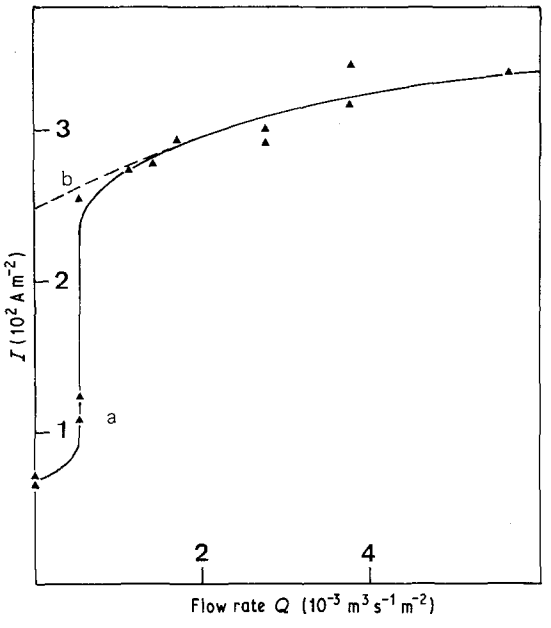


Fig. 8. Influence of the gas volumetric flow rate $Q$ on limiting current: (a) CSR; (b) PFR. Electrolytic flow = $1.29 \times 10^{-3}$ $m^3 s^{-1} m^{-2}$. 0.018 mol $dm^{-3}$ $Ph_3SnCl$ in MeOH, 0.5 M $LiClO_4$. Currents and flows are given for 1 $m^2$ of horizontal cross-section of the cathode.

This increase in $I_1$, smaller than that predicted by Equation 2, is explained by the blocking of the effective electrode area which occurs when the gas bubbles burst at the surface of the mercury. Nevertheless, increasing the nitrogen flow rate in the plug–flow reactor results, on the one hand, in an enhancement of the mass transfer coefficient $k$ by increasing the circulation rate of the electrolyte, and on the other, in an improvement in the elimination of the insoluble film of distannane. As a result, this operating mode was chosen for preparative runs (see part I).

### 6.2. *Continuously stirred reactor*

When the catholyte is fed into the reactor through the top, the bubbling of the nitrogen plays an essential role in maintaining a productivity equivalent to that of the plug–flow reactor. Fig. 8 shows the existence of a threshold in the nitrogen flow rate ($0.54 \times 10^{-3}$ $m^3 s^{-1} m^{-2}$) above which a sudden increase in limiting current appears. Beyond this threshold, the increase in current as a function of the nitrogen flow rate becomes comparable to that observed in the case of the plug–flow reactor. The threshold value corresponds to the appearance of gas bubbles bursting across the whole mercury surface. Cutting the nitrogen flow causes the current to drop immediately to a low value; this latter phenomenon is due to the masking of the whole electrode surface.

## 7. Conclusion

The purpose of this study was to test a new electrochemical reactor for use in the continuous manufacture of two distannanes: $Bu_3SnSnBu_3$ and $Ph_3SnSnPh_3$. Electrolysis tests were conducted with the solution recycling between the reactor and the separator where the insoluble distannanes were removed. Reduction of $Bu_3SnCl$ on mercury in methanol to produce the $Bu_3Sn^{\cdot}$ radical is a reaction limited by charge transfer through an adsorbed layer and a coating of insoluble hexabutyldistannane. Reduction of $Ph_3SnCl$, limited by mass transfer at concentrations below $2 \times 10^{-2}$ mol dm$^{-3}$, was used to test the mass transport characteristics of the mercury–solution interface.

The following conclusions were reached: (a) In the case of the PFR, the limiting current is related to the electrolyte flow rate by a correlation characteristic of laminar flow regimes. (b) In the case of the CSR, performances close to those of the PFR could be obtained, as long as the inert gas stream through the mercury was maintained. The plug–flow reactor, which provides a better elimination of the insoluble product formed, was finally chosen for long-term operation.

This investigation has made possible the collection of a stock of electrochemical, energetic and mass-transfer data which can be used for a theoretical estimate of the productivity of a larger electrolysis cell operating under the same conditions in the region of electrolysis. Among these results, the most valuable in the scale-up to a larger prototype are such data as the variation in overvoltage with current density for various reactant concentrations and the variation in the rate of convective mass transfer as a function of fluid velocities.

## Acknowledgements

We are grateful for financial support from the Delegation Générale à la Recherche Scientifique et Technique (Contract 75-7-1550).

## References

[1] R. E. Sioda, *Electrochim. Acta* **19** (1974) 57.
[2] D. J. Pickett, *ibid* **18** (1973) 835.
[3] A. T. S. Walker and A. A. Wragg, *ibid* **22** (1977) 1129.
[4] A. T. Kuhn and B. Marquis, *J. Appl. Electrochem.* **2** (1972) 275.
[5] D. Matic, *ibid* 9 (1979) 15.
[6] A. Savall and G. Lacoste, *Proc. 1st Mediterranean Congress on Chemical Engineering, Barcelona*, November (1978).
[7] N. Ibl, J. Venczel, E. Schalch and E. Adam, *Chemie Ing. Technol.* 43 (1971) 202.
[8] D. Jennings, A. T. Kuhn, J. B. Stepanek and R. Whitehead, *Electrochim. Acta* **20** (1975) 903.
[9] R. W. Houghton and A. T. Kuhn, *J. Appl. Electrochem.* 4 (1974) 173.
[10] K. Stephan and H. Vogt, *Electrochim. Acta* **24** (1979) 11.
[11] M. G. Fouad and G. H. Sedahmed, *ibid* **18** (1973) 55.
[12] L. J. J. Janssen and J. G. Hoogland, *ibid* **15** (1970) 1013.
[13] D. J. Pickett, 'Electrochemical Reactor Design', Elsevier, Amsterdam (1977).
[14] A. Savall and G. Lacoste, *Proc. Sixth Int. Symp. on Chemical Reaction Engineering, Nice*, March (1980).
[15] A. Savall, G. Lacoste, P. Mazerolles, *J. Appl. Electrochem.* **11** (1981) 61
[16] H. Jehring, H. Mehner and H. Kriegsmann, *J. Organometal. Chem.* **17** (1969) 53.
[17] M. Devaud and E. Laviron, *Rev. Chimie Minérale* **5** (1968) 427.
[18] M. Devaud and M. C. Langlois, *Bull. Soc. Chim. France* (1974) 2759.
[19] P. Leroux and M. Devaud, *ibid* (1974) 2763.
[20] M. Devaud and Y. Le Moullec, *Electrochim. Acta* **21** (1976) 395.
[21] M. Devaud and D. Gula, *ibid* **23** (1978) 565. (1978) 565.
[22] M. D. Booth and B. Fleet, *Anal. Chem.* **42** (1970) 825.
[23] Yu. M. Tyurin and V. N. Flerov, *Elektrokhim.* 6 (1970) 1548.
[24] R. Brdička, *Coll. Czech. Chem. Commun.* **12** (1947) 522.
[25] J. Heyrovsky and J. Kuta, 'Principles of Polarography', Academic Press, New York (1966) Ch. 16.
[26] E. Laviron, *J. Electroanal. Chem.* **52** (1974) 355.
[27] N. L. Weinberg and T. B. Reddy, *J. Amer. Chem. Soc.* **90** (1968) 91.
[28] V. G. Levich, 'Physico-Chemical Hydrodynamics', Prentice-Hall, Englewood Cliffs, New Jersey (1964).
[29] A. Karabelas, T. Wegner and T. Hanratty, *Chem. Eng. Sci.* **26** (1971) 1581.
[30] J. R. Selman and C. W. Tobias, *Adv. Chem. Eng.* **10** (1978) 211.